Timing of Ore-Related Magmatism in the Western Alaska Range, Southwestern Alaska

By Ryan D. Taylor, Garth E. Graham, Eric D. Anderson, and David Selby

Open-File Report 2014–1115

U.S. Department of the Interior
U.S. Geological Survey

U.S. Department of the Interior
SALLY JEWELL, Secretary

U.S. Geological Survey
Suzette M. Kimball, Acting Director

U.S. Geological Survey, Reston, Virginia: 2014

For more information on the USGS—the Federal source for science about the Earth, its natural and living resources, natural hazards, and the environment—visit *http://www.usgs.gov* or call 1–888–ASK–USGS

For an overview of USGS information products, including maps, imagery, and publications, visit *http://www.usgs.gov/pubprod*

To order this and other USGS information products, visit *http://store.usgs.gov*

Suggested citation:
Taylor, R.D., Graham, G.E., Anderson, E.D., and Selby, David, 2014, Timing of ore-related magmatism in the western Alaska Range, southwestern Alaska: U.S. Geological Survey Open-File Report 2014–1115, 25 p., *http://dx.doi.org/10.3133/ofr20141115*.

ISSN 2331-1258 (online)

Contents

Figures

Tables

Conversion Factors

Inch/Pound to SI

Multiply	By	To obtain
	Length	
foot (ft)	0.3048	meter (m)

SI to Inch/Pound

Multiply	By	To obtain
	Length	
centimeter (cm)	0.3937	inch (in.)
millimeter (mm)	0.03937	inch (in.)
meter (m)	3.281	foot (ft)
kilometer (km)	0.6214	mile (mi)
kilometer (km)	0.5400	mile, nautical (nmi)
meter (m)	1.094	yard (yd)

Temperature in degrees Celsius (°C) may be converted to degrees Fahrenheit (°F) as follows:
°F=(1.8×°C)+32

Timing of Ore-Related Magmatism in the Western Alaska Range, Southwestern Alaska

By Ryan D. Taylor, Garth E. Graham, Eric D. Anderson, and David Selby

Abstract

This report presents isotopic age data from mineralized granitic plutons in an area of the Alaska Range located approximately 200 kilometers to the west-northwest of Anchorage in southwestern Alaska. Uranium-lead isotopic data and trace element concentrations of zircons were determined for 12 samples encompassing eight plutonic bodies ranging in age from approximately 76 to 57.4 millions of years ago (Ma). Additionally, a rhenium-osmium age of molybdenite from the Miss Molly molybdenum occurrence is reported (approx. 59 Ma). All of the granitic plutons in this study host gold-, copper-, and (or) molybdenum-rich prospects.

These new ages modify previous interpretations regarding the age of magmatic activity and mineralization within the study area. The new ages show that the majority of the gold-quartz vein-hosting plutons examined in this study formed in the Late Cretaceous. Further work is necessary to establish the ages of ore-mineral deposition in these deposits.

Introduction

This report presents isotopic age data from mineralized granitic plutons in an area of the Alaska Range located approximately 200 kilometers (km) to the west-northwest of Anchorage in southwestern Alaska (fig. 1). These data were collected as part of the Western Alaska Range Project (WARP) funded by the U.S. Geological Survey (USGS) Mineral Resources Program with goals of defining the metallogenic setting and geologic evolution of the region. Uranium-lead (U-Pb) isotopic data and trace element concentrations of zircons were determined for 12 samples encompassing eight plutonic bodies. Additionally, a rhenium-osmium (Re-Os) age of molybdenite from the Miss Molly molybdenum occurrence is reported. All of the granitic plutons in this study host gold (Au)-, copper (Cu)-, and (or) molybdenum (Mo)-rich prospects (U.S. Geological Survey, 2008).

The western Alaska Range is rugged and remote, with no large-scale lode mines presently operating. However, initial processing of bulk high-grade gold vein ores has begun at the Terra property (Gustavson Associates, LLC, 2013). The study area lies approximately 100 km north-northeast of the large Pebble porphyry Cu-Au-Mo deposit and generally along trend with the associated mid-Cretaceous plutonic belt; this belt is the focus of ongoing regional exploration for copper and (or) gold deposits.

Historic potassium-argon (K-Ar) amphibole and mica geochronology examinations indicate that the study area is largely composed of latest Cretaceous to Paleocene plutons that intruded the Kahiltna flysch overlap succession (Reed and Lanphere, 1969, 1972, 1973). Mineral prospects spatially associated with some of these plutons, including those sampled in this study, are typically composed of low-sulfide stockwork veins, sheeted veins, disseminated ore, and (or) breccia bodies hosted within several of these intrusions and to a lesser extent within immediately surrounding hornfelsed country rock. Although direct dating of alteration and ore minerals is currently lacking, this magmatic event is considered to be related to the last of three metallogenic episodes during the Mesozoic in this part of the Alaska Range. This report provides more modern and precise crystallization age determinations of the plutons that host mineral prospects.

Methods

Uranium-Lead Zircon

Samples of the least altered igneous rocks were collected as part of helicopter-supported field work in July 2012. The locations of samples are shown in figure 1, and coordinates and sample identifications are provided in table 1. In most cases, samples were taken from bedrock, although extreme terrain necessitated rubble crop and talus sampling at some locations. A single sample was collected from a glacial train of material 100 meters (m) down-ice of but derived from an inaccessible headwall at one site within the Mt. Estelle composite pluton.

Whole rock samples were crushed, ground, and sieved to fractions 250–149 and 149–74 micrometers (µm) in size for further zircon separation. Standard density and magnetic separation techniques, including a Wilfley table, Frantz magnetic separator, and methylene iodide heavy liquids were used to concentrate zircons. Individual zircon crystals from each sample were hand-picked under a binocular microscope to ensure purity prior to being mounted into epoxy disks. The zircons were ground to approximately half the thickness of the individual crystals and then polished sequentially using 6-µm and 1-µm diamond suspension. All grains were imaged by transmitted and reflected light using a camera mounted on a petrographic microscope and by cathodoluminescence (CL) using a scanning electron microscope in the U.S. Geological Survey's Microbeam Laboratory in Denver, Colorado. The age standard zircon R33 (419 millions of years old [Ma]; Black and others, 2004) was cast into each mount along with the unknowns.

Zircon crystals were analyzed using the sensitive high-resolution ion microprobe with reverse geometry (SHRIMP-RG) at the Stanford–USGS Micro Analysis Center in Palo Alto, California. Compositional standards 91500, SL13, and MAD were analyzed from an in-house mount (Wiedenbeck and others, 1995; Black and others, 2003; Mazdab and Wooden, 2006). Uranium-lead isotopic data and trace element data were collected for each analyzed spot on a zircon crystal using the methods of Williams (1998). Raw data were reduced using the Squid 2 program (Ludwig, 2009) and plotted using Isoplot 3.75 software (Ludwig, 2012).

Spot locations for SHRIMP analysis were chosen preferentially from the most homogenous portions of the crystal rims based upon CL images. Areas of intermediate brightness were favored in order to analyze areas with ideal uranium concentrations (approximately a few hundred to three thousand parts per million). The transmitted and reflected light images were used to avoid locations with fractures, imperfections, or obvious mineral inclusions.

Titanium (Ti) concentrations of the zircons were also determined to estimate the temperature of crystallization. Total Ti was determined by measuring the concentration of ^{48}Ti because its representative isotopic component is 73.72 percent of the total Ti. These data were used to calculate zircon crystallization temperatures based on the Ti-in-zircon thermometer of Ferry and Watson (2007). Temperatures were calculated assuming TiO_2 activities of 0.7 and 0.5, with a temperature that averages roughly 35 °C greater for the lower activity value. Titanium activity within granitic melts is generally between 0.6 and 0.9 and is controlled by many Ti-bearing minerals such as rutile and sphene (Watson and others, 2006; Hayden and Watson, 2007). An activity of 1.0 for SiO_2 was also assumed based upon the presence of quartz and feldspar in the primary mineral assemblages and on their textures.

Rhenium-Osmium Molybdenite

Multiple samples of quartz-molybdenite±fluorite veins that cross-cut granite were collected from the Miss Molly prospect in July 2011. Three samples of quartz vein and adjacent rock containing molybdenite were crushed and sieved. Material sieved to 841–250 and 250–149 µm in size was cleaned in acetone to remove dust and clay particles. Heavy liquid separation using methylene iodide segregated the denser sulfides from the light silicates. Molybdenite crystals were handpicked from the sulfide concentrate under a binocular microscope to ensure purity. Three molybdenite aliquots were analyzed at Durham University, England, for Re-Os isotopic and concentration data following the analytical protocol of Selby and others (2007).

Whole Rock Sample Descriptions

Elevated SiO_2 activity and the felsic nature of all granitic samples are indicated by the presence of quartz and feldspar in primary assemblages. The composite Mt. Estelle pluton was sampled at five locations associated with different mineral occurrences. Photographs of samples and sample sites are found in the appendix.

12WA01RT—Mt. Estelle Pluton—Oxide Valley Gold Prospect

The Oxide Valley sample was collected from a granitic outcrop near the headwall of the valley. The outcrop contains irregularly distributed oblate mafic enclaves, although these were not sampled. Chalcopyrite and arsenopyrite occur on some fracture surfaces of the outcrop.

The sample is medium-grained and slightly porphyritic, with plagioclase and biotite phenocrysts that are up to 1.5 centimeters (cm) and 3–4 millimeters (mm) in size, respectively. The majority of the matrix crystals are 1–4 mm in size.

12WA07RT—Mt. Estelle Pluton—Train Gold Prospect

The Train prospect sample was collected from a progression of glacial material derived from an inaccessible headwall approximately 100 m up-ice. The sample’s color is grey to melanocratic and its texture is aphyric. Most crystals are a few millimeters in size with quartz and feldspar crystals displaying a greenish tint in hand specimens. Dark, mafic minerals include biotite and hornblende.

12WA11RT—Snow Ridge Porphyry Prospect

A visibly least altered sample from Snow Ridge was collected tens of meters up a ridge from quartz-carbonate-pyrite-sphalerite-galena veins exposed along a small creek. The sampled material was derived from both outcrop and rubble crop. The rock becomes progressively more altered closer to the ore-bearing veins. This prospect has a similar geochemical signature to that of the Whistler porphyry Cu-Au-Mo deposit located within a few kilometers to the south of Snow Ridge.

Abundant plagioclase phenocrysts up to 9 mm in length occur within a dark matrix of crystals mostly <1 mm in size. It is melanocratic with the obvious white plagioclase phenocrysts peppered throughout. Feldspar phenocrysts and much of the matrix are altered to carbonate and sericite. Compared with other samples from this study, this sample contains abundant sphene but less quartz.

12WA13RT—Cristo Gold-Copper Prospect Area

The sample from near the Cristo prospect was collected in the eastern drainage of the prospect, and although the sample is altered, it was the best available. The rock is pink, in contrast to more altered and bleached samples from the area which have thin quartz veinlets throughout. It is not porphyritic. Average grain size is <2 mm, except for larger late-stage quartz and potassium feldspar crystals filling in open-space vugs and cavities. Chlorite occurs in some of the vugs.

12WA15RT—Distin Pluton Gold Prospect

This unaltered sample was collected from an outcrop of the Distin pluton. Easily accessible samples of mineralized rock were not available from the outcrop but were abundant as quartz-arsenopyrite vein fragments and veins in intrusive rock in the talus field derived from outcrop. The sample is equigranular, with crystals <2 mm and mostly around 1 mm in size. The biotite-rich nature of the sample creates a grey color.

12WA17RT—Terra Gold Deposit

The Terra sample was collected from core hole WGC 11-34B between the depths of 333.5 and 340.5 feet. It is part of a diorite dike (?) that is approximately 150 m thick and 1.8 km long, which hosts localized bonanza-grade gold-bearing quartz veins of the Terra deposit (Gustavson Associates, LLC, 2013). The diorite is cut by chlorite veins, but these and the immediately adjacent diorite were removed from our sample prior to processing.

Grain size in this pyroxene-bearing melanocratic rock is 1–3 mm. This sample is more mafic than other samples from this study.

12WA25RT—Old Man Diorite Gold Prospect

A sample from the Old Man diorite was collected from an outcrop that contains irregular zones of numerous quartz and carbonate veins with little to no sulfide mineralization. The analyzed sample was distal from veins and was less altered than much of the large outcropping area.

Plagioclase phenocrysts range from 2–7 mm within a matrix of crystals <1 mm in size, which imparts a slightly porphyritic texture to the sample.

12WA26RT—Mt. Estelle Pluton—Muddy Creek Gold-Copper Prospect

Talus at the bottom of a cirque and headwall of the Mt. Estelle pluton was sampled at the Muddy Creek prospect. Chalcopyrite veinlets within fractures and disseminated chalcopyrite produced rust spots on weathered surfaces on scattered talus in the region. Oxidized and weathered surfaces contained malachite. The majority of the veins are composed of quartz with lesser amounts of barren calcite veins.

The sampled material is medium- to coarse-grained and displays salt-and-pepper coloring. A few potassium feldspar phenocrysts are as large as 1 cm in length. Non-feldspar crystals are generally <1 mm in size. It is relatively fresh, with pristine biotite but chloritized hornblende.

12WA27RT—Jimmy Lake Polymetallic Prospect

The sample from the Jimmy Lake base metal prospect was collected from a talus field consisting of 100 percent intrusive boulders derived from a headwall far up the hillside. This porphyritic sample is leucocratic with 3- to 10-mm quartz and potassium feldspar phenocrysts within a matrix of crystals <1.5 mm in size. Minor amounts of biotite constitute the mafic silicate phase.

12WA28RT—Unnamed "Orange Ridge" Copper-Silver-Gold Prospect

A sample from an unnamed prospect, herein referred to informally as "Orange Ridge," was collected from rubble crop at the top of a rounded peak. Sizable outcrops of the intrusive material were lacking. The sample is a least altered example of extensively sericitized and silicified, strongly orange-colored intrusive rock. Minor quartz veins containing arsenopyrite, chalcopyrite, and pyrite were observed to cut the intrusive rock. The selected sample was barren of sulfides and quartz veins.

The sample has a seriate texture. The largest crystals are feldspars; all crystals, including the feldspars, quartz, and biotite, range from <1 to 5 mm in size.

12WA31RT—Mt. Estelle Pluton—RPM Gold-Copper Prospect

Outcrops at the RPM prospect within the composite Mt. Estelle pluton were sampled. All of the intrusive rock in this area is at least partially altered, but this sample was selected because field observations indicated it was relatively less altered. In addition to quartz veining, the area also features pegmatite veins containing sulfide minerals and tourmaline.

Except for the 1- to 2-mm biotite crystals, this sample is leucocratic. Feldspar crystals as large as 5–10 mm impart a slight porphyritic texture.

12WA33RT—Mt. Estelle Pluton—Oxide North Gold Prospect

The unaltered sample was taken from a talus field within a cirque. Similar unaltered but mineralized samples containing disseminated pyrrhotite and chalcopyrite were observed in adjacent talus blocks. Veining is sparse in this locality. Quartz augen and feldspar are the largest crystals (up to 3 mm in length).

MM-11—Miss Molly Molybdenum Prospect

The granitic stock associated with the Miss Molly occurrence is located within hornfelsed siltstone of the Kahiltna flysch. Unaltered to least altered granite is leucocratic and composed of coarse grained potassium feldspar, quartz, plagioclase, biotite, and other trace minerals such as apatite and zircon. It is equigranular and not porphyritic.

Vein mineralization occupies dilatant fractures (Fernette and Cleveland, 1984). The quartz veins contain fluorite, molybdenite, pyrite, chalcopyrite, and mica. Molybdenite also occurs as smears along fractures and as disseminations within the granite.

Results

Age summaries of the samples are provided in table 1. Uranium-lead ages calculated for zircon and Re-Os ages for molybdenite are described, and a pluton age comparison between ages calculated for this study and historic K-Ar ages is discussed. Zircon U-Pb ages are presented on conventional concordia diagrams (Wetherill, 1956) that compare radiogenic Pb values with their respective radioactive U isotopes for purposes of defining an age of formation and as weighted average ages for individual crystals from each sample location.

Zircon

Uranium-lead isotopic values are presented in tables 1–2 and figures 2–13. Individual crystals separated from whole-rock samples collected at each sample location are identified in tables 2 and 3. Preferred ages are ^{207}Pb-corrected ^{206}Pb/^{238}U (Ireland and Williams, 2003); the ages provided in table 1 are weighted average ages. A ^{207}Pb-corrected age is preferred for relatively young (Cretaceous or younger in this case) crystals because the analyzed zircons contain essentially no ^{204}Pb and because discordance of Phanerozoic crystals in individual analyses is typically not detectable within the limits of analytical uncertainty (Ireland and Williams, 2003). The zircons from each sample except Jimmy Lake represent distinct single populations with no xenocrysts or outliers reported. Samples from the Jimmy Lake and Cristo prospects yielded the youngest ages of 57.4 Ma and 57.8 Ma, respectively. The oldest sample is from Snow Ridge with an age of 76.6 Ma. All of the other samples ranged from 70.8 to 66.7 Ma, with two modes at approximately 68 and 71–70 Ma (fig. 14). The composite Mt. Estelle pluton had samples of distinct magmatic phases that ranged in age from 70.1 to 66.7 Ma.

Data from the Jimmy Lake sample include two different populations of zircon. The youngest population is reported in table 1 and figure 10 with an age of 57.4 Ma. The older population has a calculated age of 61.5 Ma based upon 5 zircon crystals.

Trace element and Ti-in-zircon geothermometry results are listed in table 3. Average calculated temperatures of crystallization using a TiO_2 activity of 0.7 is between 668 and 891 °C. Temperatures calculated for individual crystals using a TiO_2 activity of 0.7 ranged from 618 to 951 °C, excluding a single outlier with an unrealistically high calculated temperature (crystal 11RT-12 from Snow Ridge). This single analysis was elevated because of a Ti-Fe-oxide inclusion that was under the beam during the analysis.

Rhenium-Osmium

Only one of the three molybdenite samples (MM-11) from the Miss Molly occurrence contained sufficient Re to provide an age date (table 4). This sample contained 141 parts per billion (ppb) Re and yielded an age of 58.5±1.2 Ma. The two other molybdenite samples contained less than 10 ppb Re, concentrations insufficient to override the signal from the blank. These two molybdenite aliquots were too small and contained too little Re to produce accurate data. To our knowledge, these concentrations of Re are the lowest reported in molybdenite to date.

Pluton Age Comparison

Previous interpretations of plutonic activity in the region based upon K-Ar geochronology suggested that magmatic activity began in the Late Cretaceous (at approx. 76 Ma) but that the bulk of the intrusive activity occurred in the Paleocene (between 65 and 59 Ma;

fig. 14). A few younger K-Ar dates extend into the Oligocene (as young as 25.5 Ma). The K-Ar age data, however, did not focus on plutonic bodies that are spatially associated with base and precious metal mineralization. The new ages show that the majority of the gold-quartz vein-hosting plutons formed in the Late Cretaceous (71–66 Ma; fig 14).

Four of the eight plutons or nearby mapped equivalents (Reed and Elliot, 1970; Reed and Nelson, 1980) dated by U-Pb in this study were previously dated by K-Ar (fig. 14; Reed and Lanphere, 1972, 1973). The new age results show that the composite Mt. Estelle pluton and the diorite dike(?) related to the Terra deposit are older than previously interpreted by 4 million years (m.y.) and 7 m.y., respectively. The Distin pluton complex has similar K-Ar and U-Pb ages but are approximately 1.5 m.y. older based upon the zircon crystallization age. "Orange Ridge" plutonism is approximately 3.5 m.y. younger than suggested by K-Ar geochronology. These results that employ the more robust U-Pb dating technique indicate that these gold-quartz vein-hosting plutons formed during a relatively brief period of time (magmatic pulse) in latest Cretaceous (71–66 Ma; fig. 14). Younger (approx. 57 Ma) plutonic rocks at Jimmy Lake and Miss Molly contain base metal occurrences and may reflect a distinct, younger metallogenic event in this area. Further work is necessary to establish the ages of ore-mineral deposition in these deposits.

Acknowledgments

Other scientists participating in this project include, in no particular order, Richard Goldfarb, Chris Holm-Denoma, Barnaby Rockwell, Richard Saltus, Robert Ayuso, Dwight Bradley, Peter Haeussler, Jamey Jones, Julie Dumoulin, Susan Karl, Richard Lease, Erin Todd, Stephen Box, and Evan Thoms. WestMountain Gold, Millrock, and Kiska Metals generously allowed access to their properties for sampling. Jorge Vazquez provided instruction, advice, and assistance during SHRIMP data collection. Helpful reviews by Karen Kelley, Richard Saltus, and Chris Holm-Denoma improved the original manuscript.

References Cited

Black, L.P., Kamo, S.L., Allen, C.M., Davis, D.W., Aleinikoff, J.N., Valley, J.W., Mundil, Roland, Campbell, I.H., Korsch, R.J., Williams, I.S., and Foudoulis, Chris, 2004, Improved $^{206}Pb/^{238}U$ microprobe geochronology by the monitoring of a trace-element-related matrix effect—SHRIMP, ID-TIMS, ELA-ICP-MS and oxygen isotope documentation for a series of zircon standards: Chemical Geology, v. 205, p. 115–140.

Black, L.P., Kamo, S.L., Williams, I.S., Mundil, Roland, Davis, D.W., Korsch, R.J., and Foudoulis, Chris, 2003, The application of SHRIMP to Phanerozoic geochronology—A critical appraisal of four zircon standards: Chemical Geology, v. 200, p. 171–188.

Fernette, Gregory, and Cleveland, Gaylord, 1984, Geology of the Miss Molly molybdenum prospect, Tyonek C-6 quadrangle, Alaska, chap. G *of* Short notes on Alaskan geology 1982–83: Alaska Division of Geological and Geophysical Surveys Professional Report 86G, p. 35–41.

Ferry, J.M., and Watson, E.B., 2007, New thermodynamic models and revised calibrations for the Ti-in-zircon and Zr-in-rutile thermometers: Contributions to Mineralogy and Petrology, v. 154, p. 429–437.

Gustavson Associates, LLC, 2013, NI 43-101 technical report on resources, Terra Gold project, McGrath District, AK: Prepared for WestMountain Gold, Inc., endorsed by Black, Z.J., and Hulse, D.E., 123 p.

Hayden, L.A., and Watson, E.B., 2007, Rutile saturation in hydrous siliceous melts and its bearing on Ti-thermometry of quartz and zircon: Earth and Planetary Science Letters, v. 258, p. 561–568.

Ireland, T.R., and Williams, L.S., 2003, Considerations in zircon geochronology by SIMS: Reviews in Mineralogy and Geochemistry, v. 53, p. 215–241.

Ludwig, K.R., 2009, Squid 2—A user's manual, rev. 2.50: Berkeley Geochronology Center Special Publication 5, 110 p.

Ludwig, K.R., 2012, User's manual for Isoplot 3.75—A geochronological toolkit for Microsoft Excel: Berkeley Geochronology Center Special Publication 5, 75 p.

Mazdab, F.M., and Wooden, J.L., 2006, Trace element analysis in zircon by ion microprobe (SHRIMP-RG)—Technique and applications [abs.]: Geochimica et Cosmochimica Acta, v. 70, no. 18 supplement, p. A405.

Reed, B.L., and Elliott, R.L., 1970, Reconnaissance geologic map, analyses of bedrock and stream-sediment samples, and an aeromagnetic map of parts of the southern Alaska Range: U.S. Geological Survey Open-File Report 70–271, 145 p., 4 sheets, scale 1:125,000.

Reed, B. L., and Lanphere, M.A., 1969, Age and chemistry of Mesozoic and Tertiary plutonic rocks in south-central Alaska: Geological Society of America Bulletin, v. 80, p. 23–44.

Reed, B. L., and Lanphere, M.A., 1972, Generalized geologic map of the Alaska-Aleutian Range batholith showing potassium-argon ages of the plutonic rocks: U.S. Geological Survey Miscellaneous Field Studies Map 372, 2 sheets.

Reed, B.L., and Lanphere, M.A., 1973, Alaska-Aleutian Range batholith—Geochronology, chemistry, and relation to circum-Pacific plutonism: Geological Society of America Bulletin, v. 84, p. 2583–2610.

Reed, B.L., and Nelson, S.W., 1980, Geologic map of the Talkeetna Quadrangle, Alaska: U.S. Geological Survey Miscellaneous Investigations Series Map 1174, 15 p., 1 sheet, scale 1:250,000.

Selby, David, Creaser, R.A., Stein, H.J., Markey, R.J., and Hannah, J.L., 2007, Assessment of the 187Re decay constant by cross calibration of Re-Os molybdenite and U-Pb zircon chronometers in magmatic ore systems: Geochimica et Cosmochimica Acta, v. 71, p. 1999–2013.

U.S. Geological Survey, 2008, Alaska Resource Data File (ARDF): U.S. Geological Survey Open-File Report 2008–1225, accessed April 17, 2013, at *http://tin.er.usgs.gov/ardf/*.

Watson, E.B., Wark, D.A., and Thomas, J.B., 2006, Crystallization thermometers for zircon and rutile: Contributions to Mineralogy and Petrology, v. 151, p. 413–433.

Wetherill, G.W., 1956, Discordant uranium-lead ages: Transactions of the American Geophysical Union, v. 37, p. 320–326.

Wiedenbeck, M., Alle, P., Corfu, F., Griffin, W.L., Meier, M., Oberli, F., Von Quadt, A., Roddick, J.C., and Speigel, W., 1995, Three natural zircon standards for U-Th-Pb, Lu-Hf, trace element and REE analyses: Geostandards Newsletter, v. 19, p. 1–23.

Williams, I.S., 1998, U-Th-Pb geochronology by ion microprobe, *in* McKibben, M.A., Shanks, W.C., III, and Ridley, W.I., eds., Applications of microanalytical techniques to understanding mineralizing processes: Society of Economic Geologists, Reviews in Economic Geology, v. 7, p. 1–35.

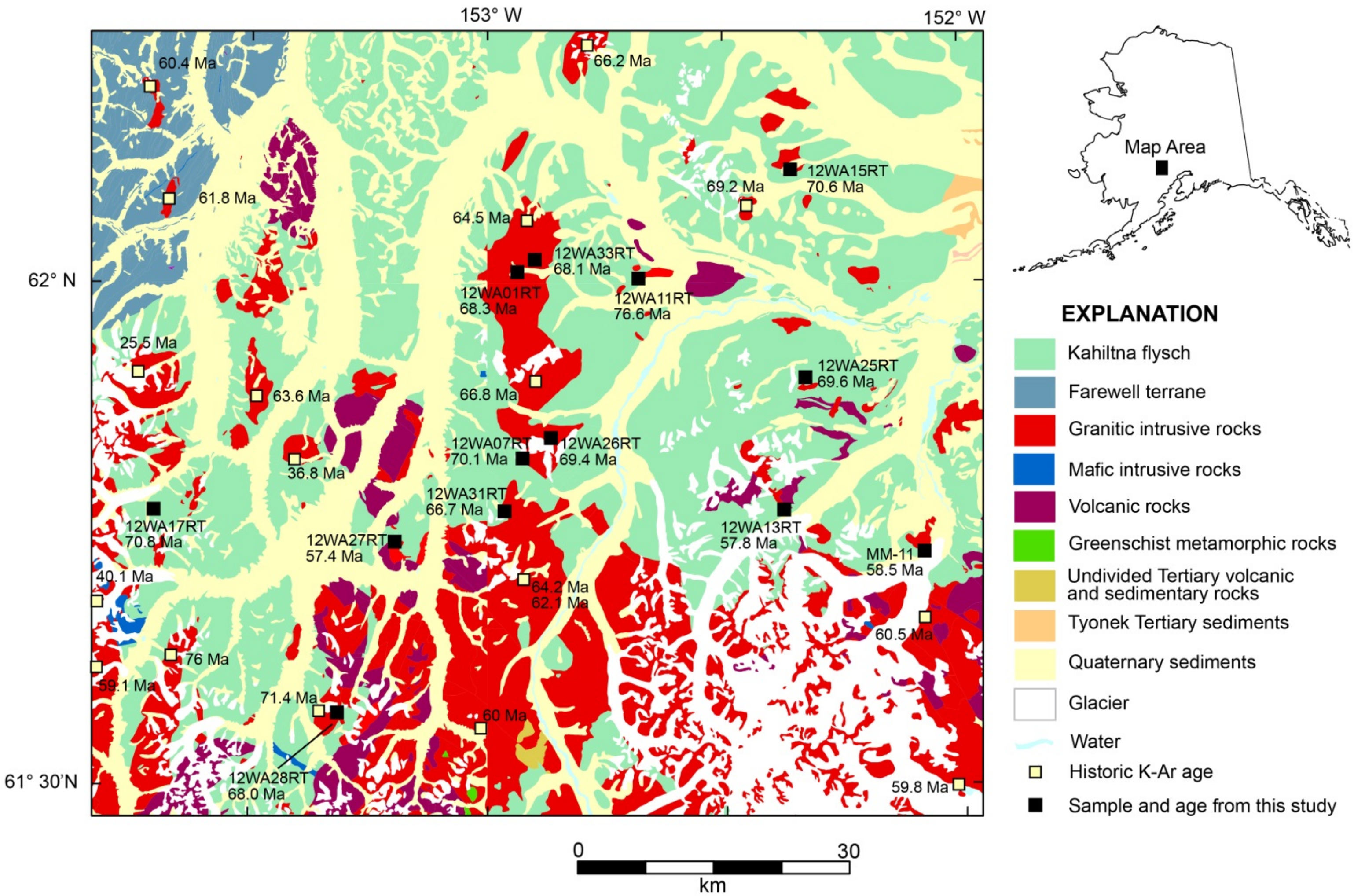

Figure 1. Simplified geologic map of the study area in the Alaska Range, Alaska, with sample locations. Note that the contacts between adjoining plutons are not shown and individual intrusions cannot be differentiated based upon this map except for those that are spatially isolated. Previous potassium-argon (K-Ar) ages of intrusive rocks in the area are included (Reed and Lanphere, 1972, 1973). Map modified from Reed and Elliot (1970) and Reed and Nelson (1980). (Ma, millions of years ago [mega-annum])

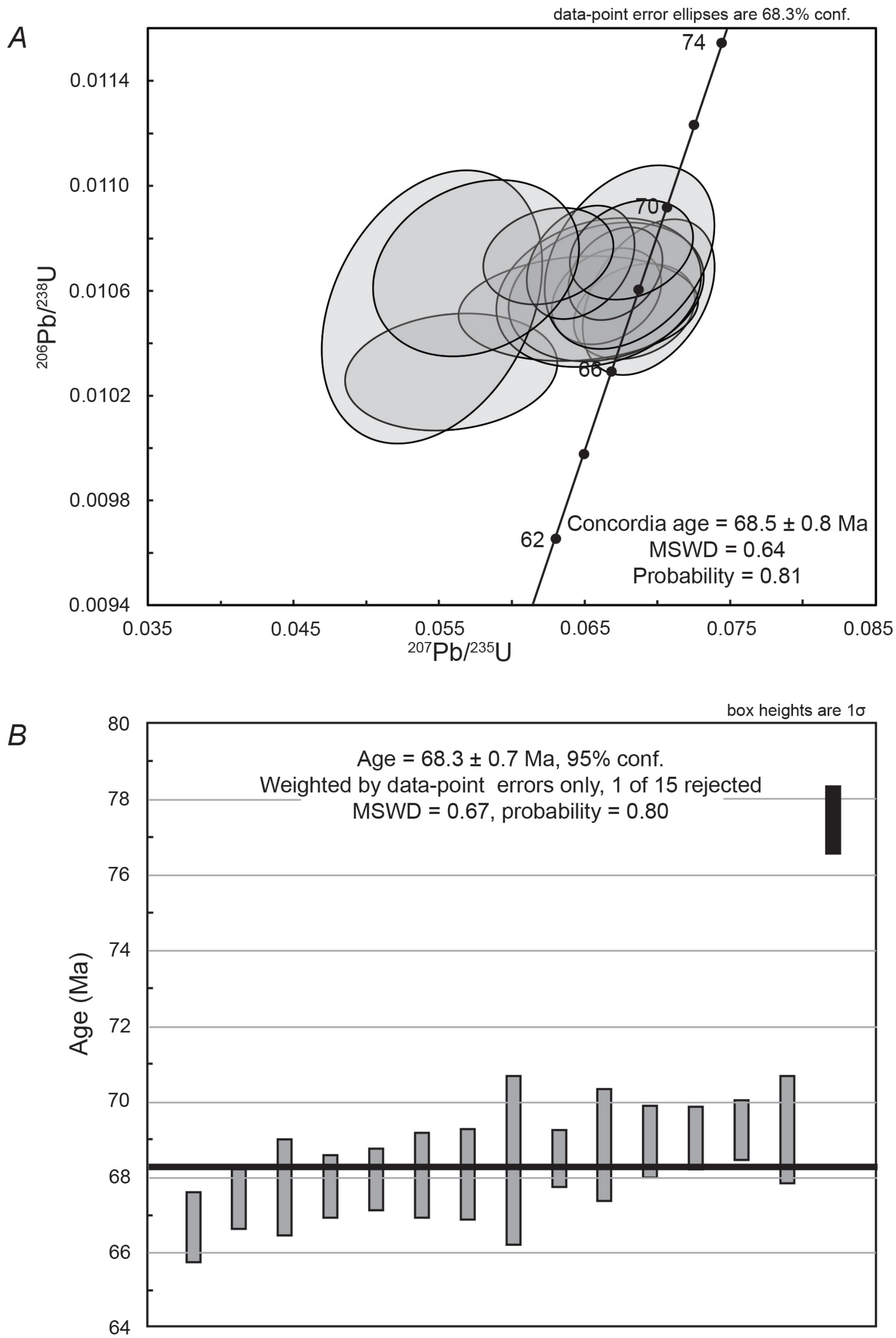

Figure 2. Uranium-lead (U-Pb) age data for zircons of sample 12WA01RT from the Oxide Valley mineral occurrence hosted within the Mt. Estelle pluton. *A*, Conventional concordia plot showing data for 14 zircon crystals. *B*, ^{207}Pb-corrected $^{206}Pb/^{238}U$ weighted-average age plot for the same zircons presented in part *A*. The black box represents an analysis that was rejected in the age determination. (Ma, millions of years ago [mega-annum]; MSWD, mean square weighted deviation; conf., confidence interval; σ, sigma [standard deviation])

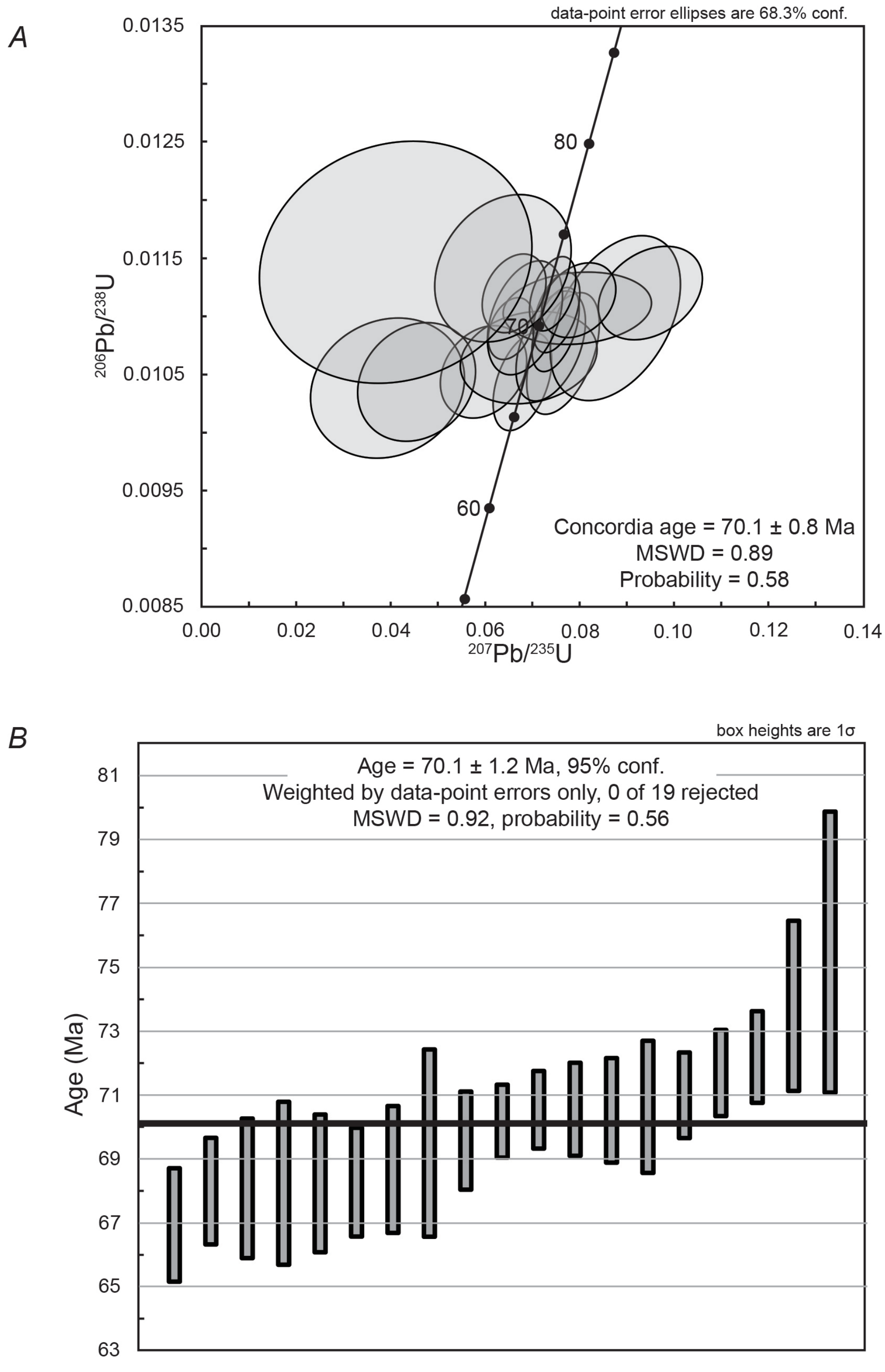

Figure 3. Uranium-lead (U-Pb) age data for zircons of sample 12WA07RT from the Train mineral occurrence hosted within the Mt. Estelle pluton. *A*, Conventional concordia plot showing data for 19 zircon crystals. *B*, ^{207}Pb-corrected $^{206}Pb/^{238}U$ weighted-average age plot for the same zircons presented in part *A*. (Ma, millions of years ago [mega-annum]; MSWD, mean square weighted deviation; conf., confidence interval; σ, sigma [standard deviation])

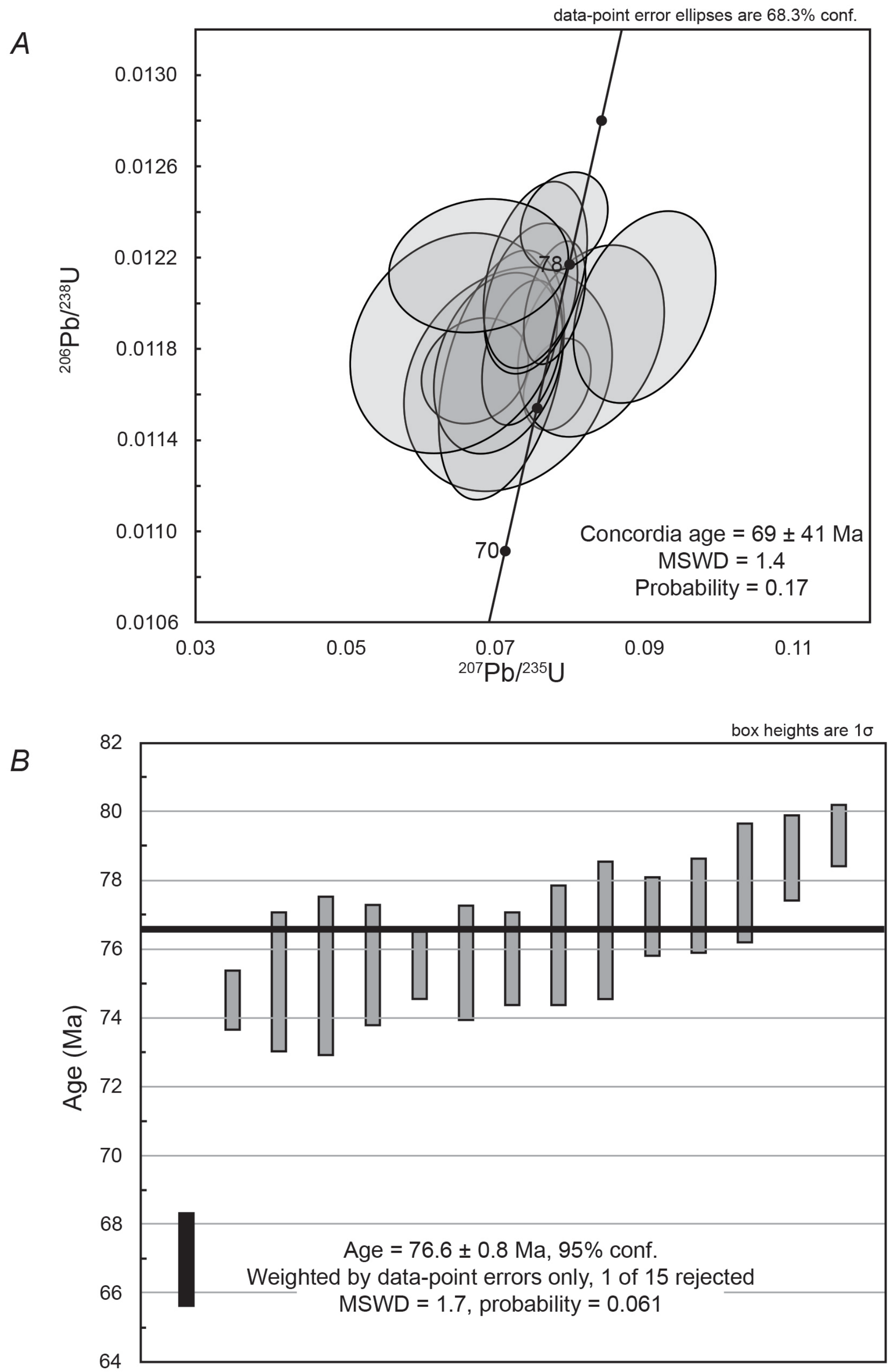

Figure 4. Uranium-lead (U-Pb) age data for zircons of sample 12WA11RT from the Snow Ridge mineral occurrence hosted within diorite. *A*, Conventional concordia plot showing data for 14 zircon crystals. *B*, ^{207}Pb-corrected $^{206}Pb/^{238}U$ weighted-average age plot for the same zircons presented in part *A*. The black box represents an analysis that was rejected in the age determination. (Ma, millions of years ago [mega-annum]; MSWD, mean square weighted deviation; conf., confidence interval; σ, sigma [standard deviation])

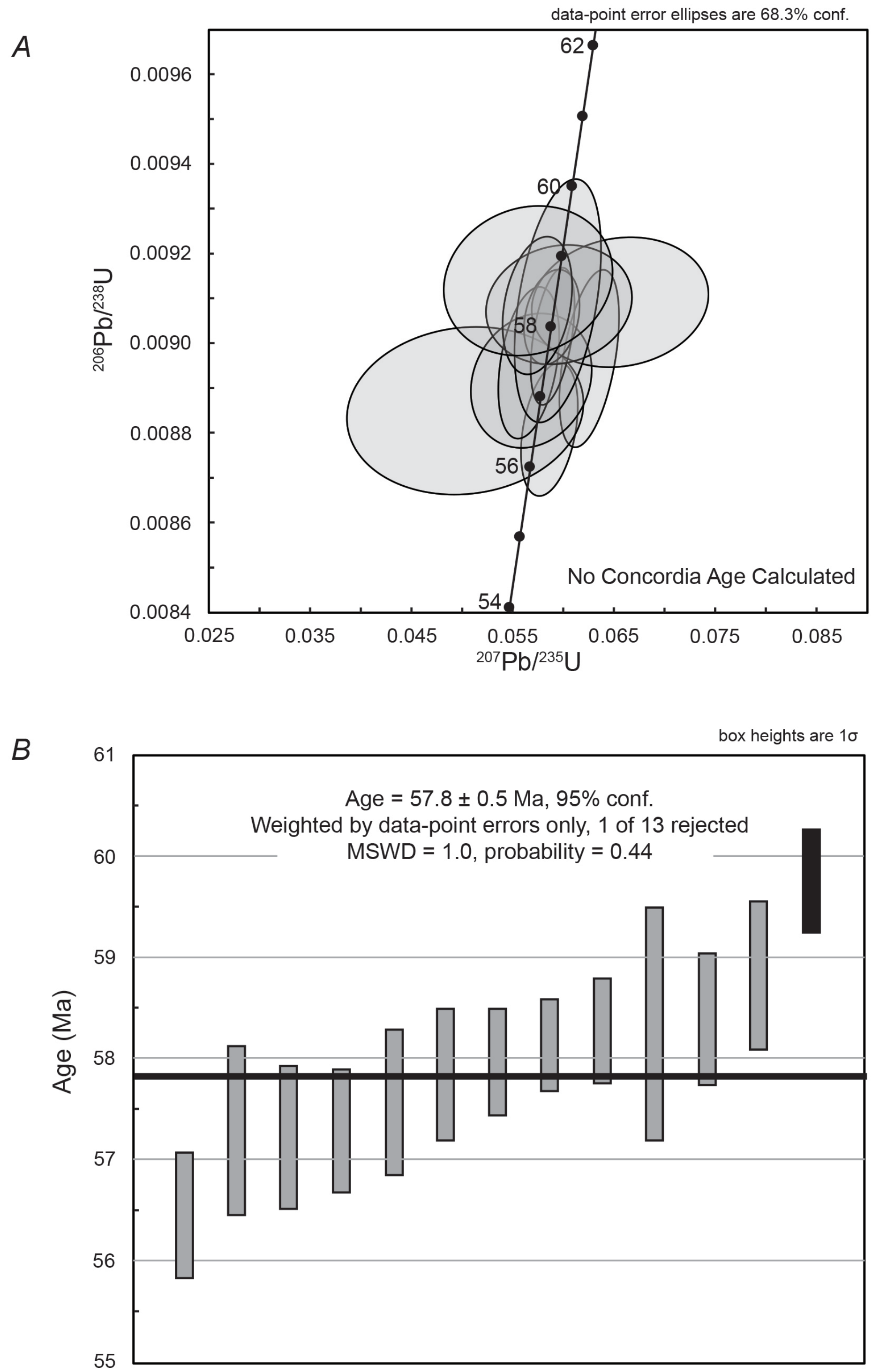

Figure 5. Uranium-lead (U-Pb) age data for zircons of sample 12WA13RT from the Cristo mineral occurrence hosted within a granitoid. *A*, Conventional concordia plot showing data for 12 zircon crystals. *B*, ^{207}Pb-corrected $^{206}Pb/^{238}U$ weighted-average age plot for the same zircons presented in part *A*. The black box represents an analysis that was rejected in the age determination. (Ma, millions of years ago [mega-annum]; MSWD, mean square weighted deviation; conf., confidence interval; σ, sigma [standard deviation])

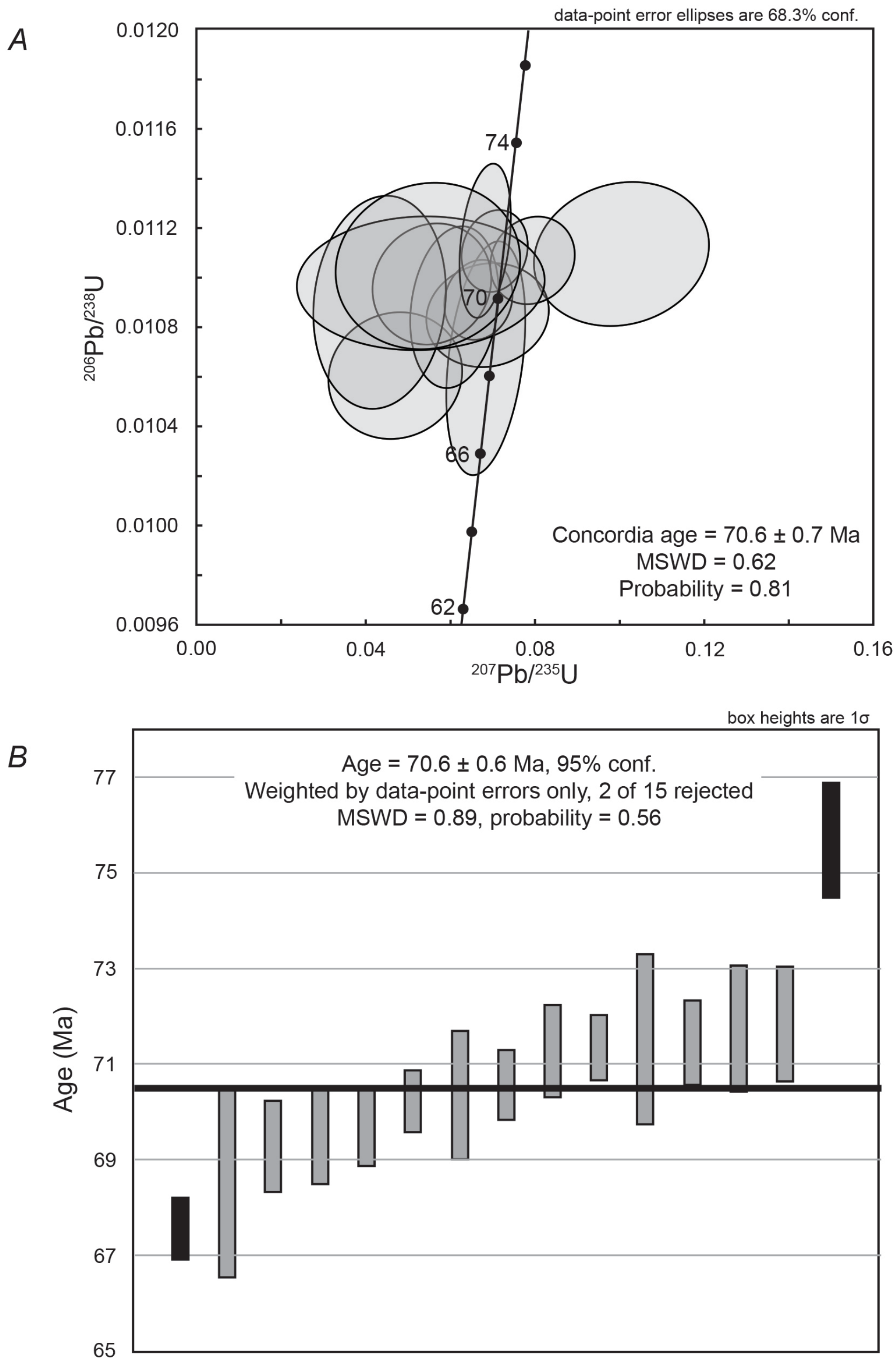

Figure 6. Uranium-lead (U-Pb) age data for zircons of sample 12WA15RT from the Distin pluton mineral occurrence. *A*, Conventional concordia plot showing data for 13 zircon crystals. *B*, ^{207}Pb-corrected $^{206}Pb/^{238}U$ weighted-average age plot for the same zircons presented in part *A*. The two black boxes represent analyses that were rejected in the age determination. (Ma, millions of years ago [mega-annum]; MSWD, mean square weighted deviation; conf., confidence interval; σ, sigma [standard deviation])

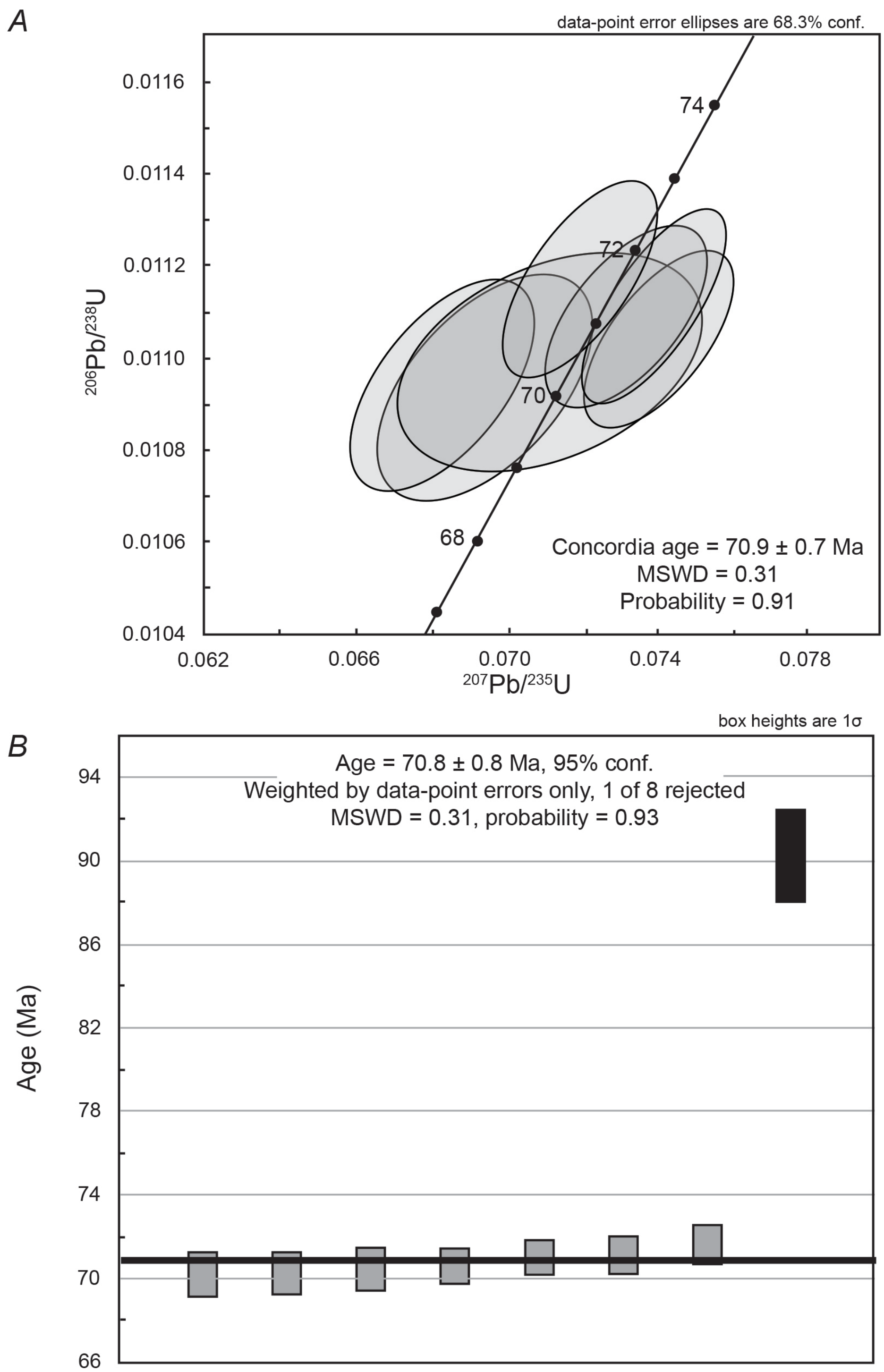

Figure 7. Uranium-lead (U-Pb) age data for zircons of sample 12WA17RT from the Terra gold deposit hosted in the Terra diorite. *A*, Conventional concordia plot showing data for 7 zircon crystals. *B*, ^{207}Pb-corrected $^{206}Pb/^{238}U$ weighted-average age plot for the same zircons presented in part *A*. The black box represents an analysis that was rejected in the age determination. (Ma, millions of years ago [mega-annum]; MSWD, mean square weighted deviation; conf., confidence interval; σ, sigma [standard deviation])

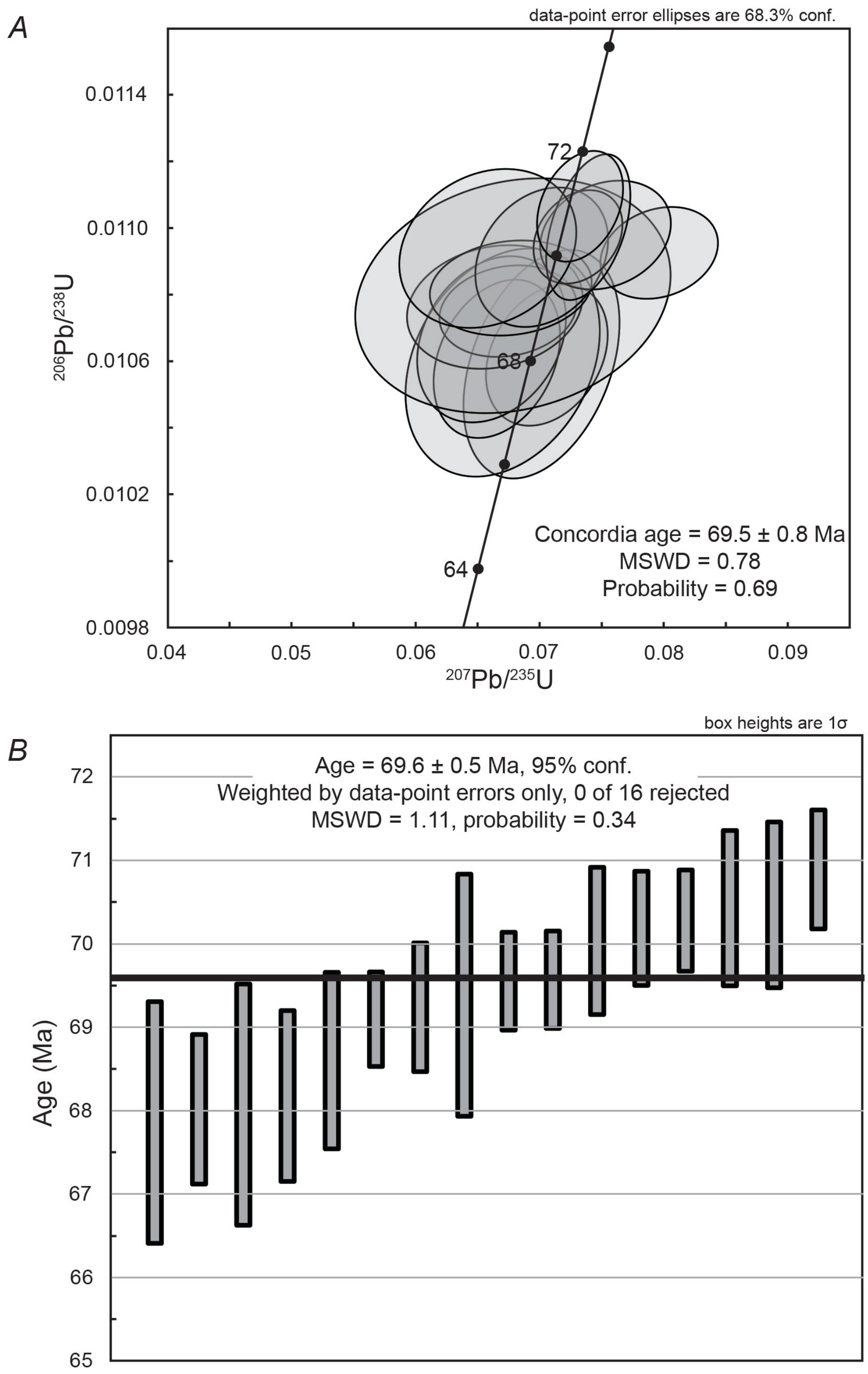

Figure 8. Uranium-lead (U-Pb) age data for zircons of sample 12WA25RT from the Old Man diorite mineral occurrence hosted in diorite. *A*, Conventional concordia plot showing data for 16 zircon crystals. *B*, ^{207}Pb-corrected $^{206}Pb/^{238}U$ weighted-average age plot for the same zircons presented in part *A*. (Ma, millions of years ago [mega-annum]; MSWD, mean square weighted deviation; conf., confidence interval; σ, sigma [standard deviation])

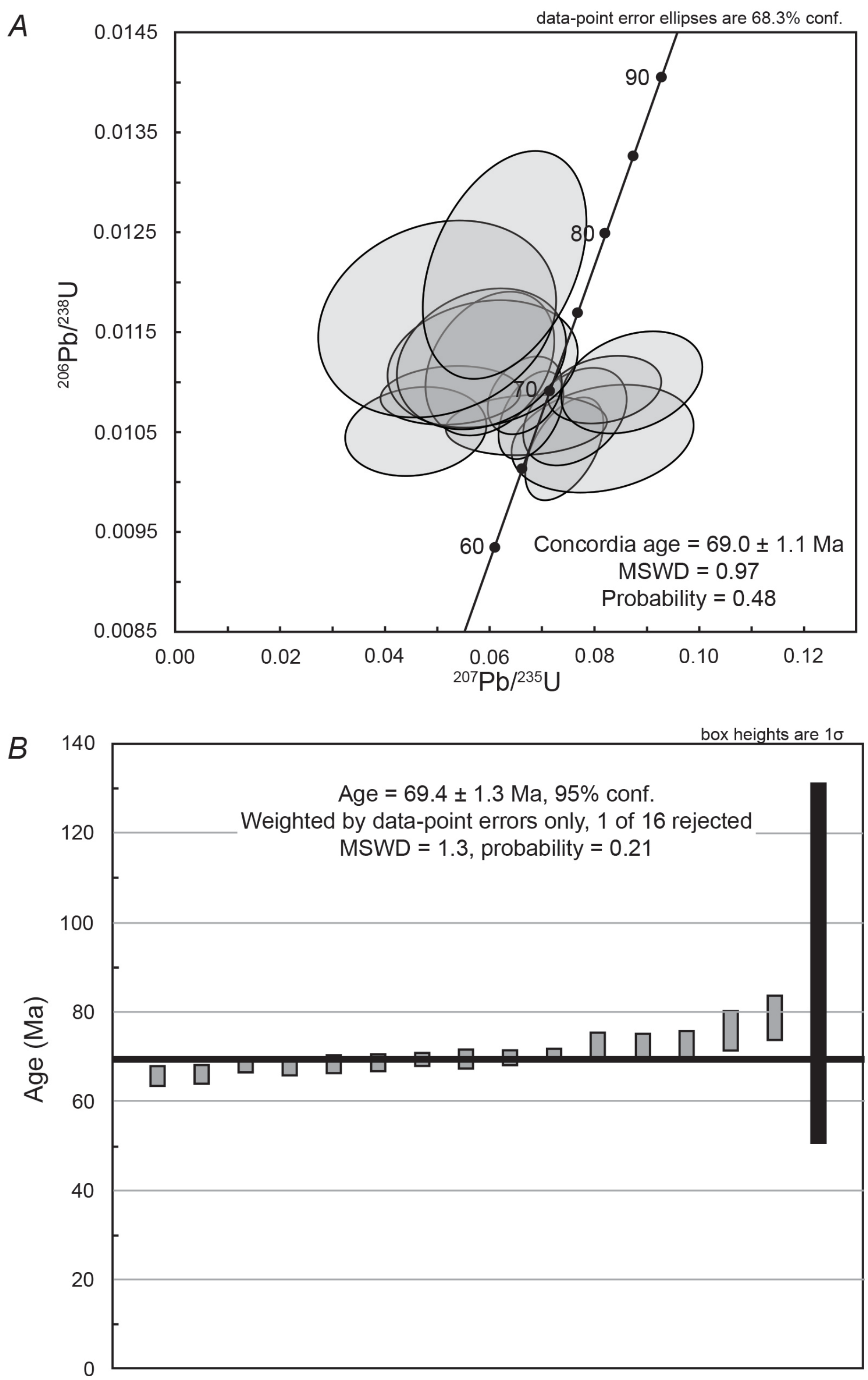

Figure 9. Uranium-lead (U-Pb) age data for zircons of sample 12WA26RT of the Muddy Creek mineral occurrence hosted in the Mt. Estelle pluton. *A*, Conventional concordia plot showing data for 15 zircon crystals. *B*, ^{207}Pb-corrected $^{206}Pb/^{238}U$ weighted-average age plot for the same zircons presented in part *A*. The black box represents an analysis that was rejected in the age determination. (Ma, millions of years ago [mega-annum]; MSWD, mean square weighted deviation; conf., confidence interval; σ, sigma [standard deviation])

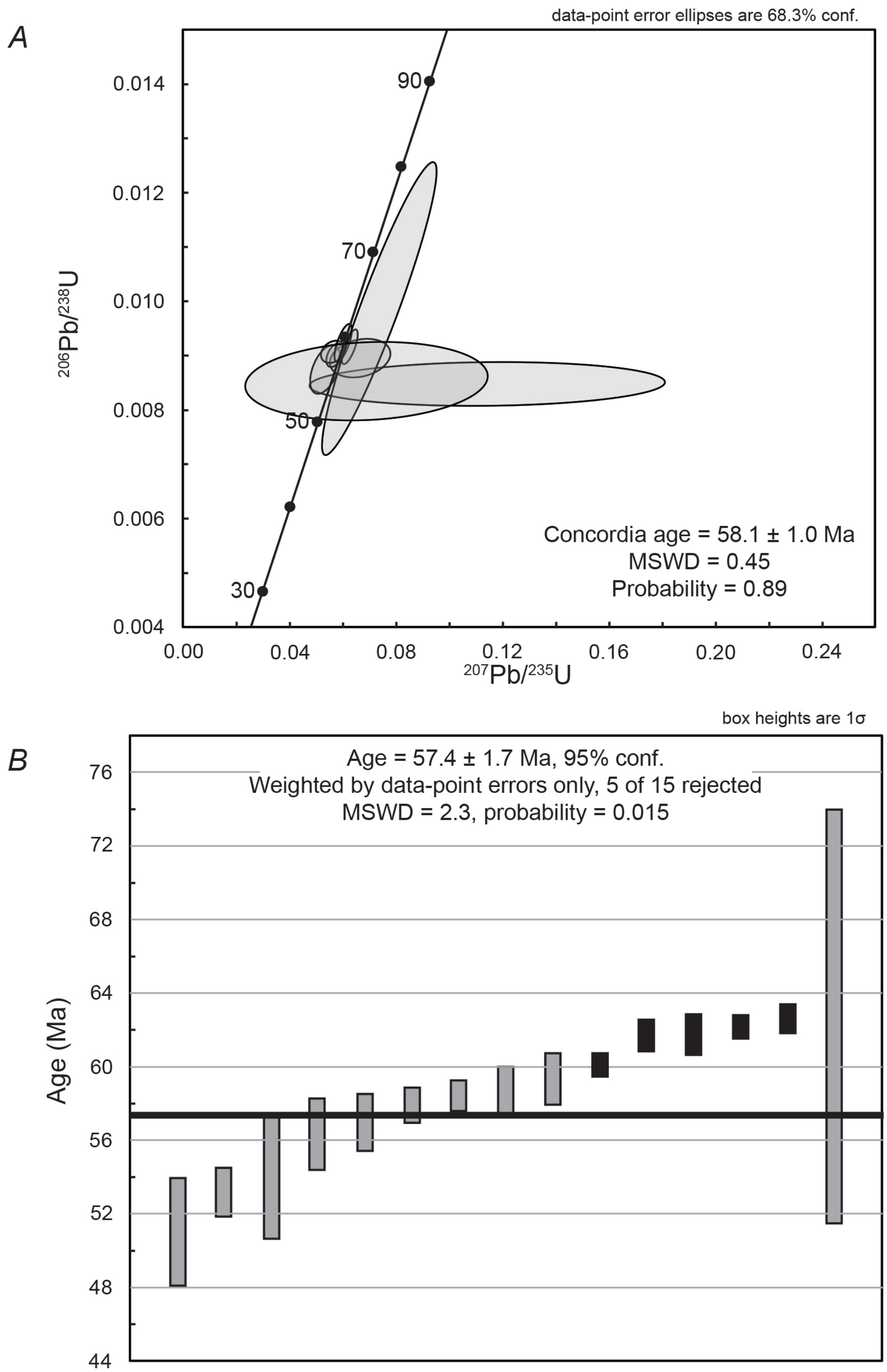

Figure 10. Uranium-lead (U-Pb) age data for zircons of sample 12WA27RT of the Jimmy Lake molybdenum occurrence hosted in granite. *A*, Conventional concordia plot showing data for 10 zircon crystals. *B*, ^{207}Pb-corrected $^{206}Pb/^{238}U$ weighted-average age plot for the same zircons presented in part *A*. The black boxes represent analyses that were rejected in the age determination because they represent a different population of zircons. (Ma, millions of years ago [mega-annum]; MSWD, mean square weighted deviation; conf., confidence interval; σ, sigma [standard deviation])

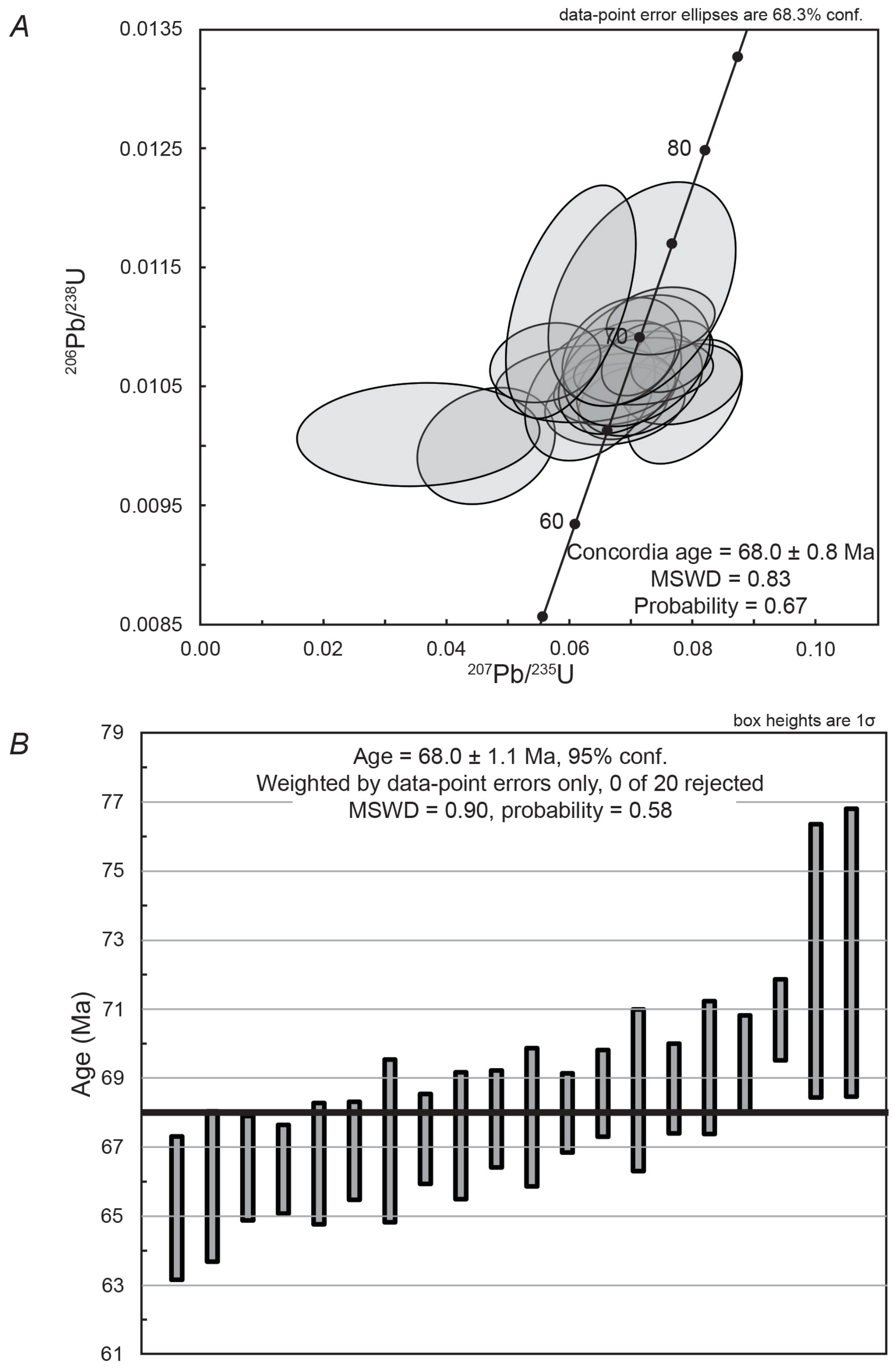

Figure 11. Uranium-lead (U-Pb) age data for zircons of sample 12WA28RT from the “Orange Ridge” mineral occurrence hosted within granitoid. *A*, Conventional concordia plot showing data for 20 zircon crystals. *B*, ^{207}Pb-corrected $^{206}Pb/^{238}U$ weighted-average age plot for the same zircons presented in part *A*. (Ma, millions of years ago [mega-annum]; MSWD, mean square weighted deviation; conf., confidence interval; σ, sigma [standard deviation])

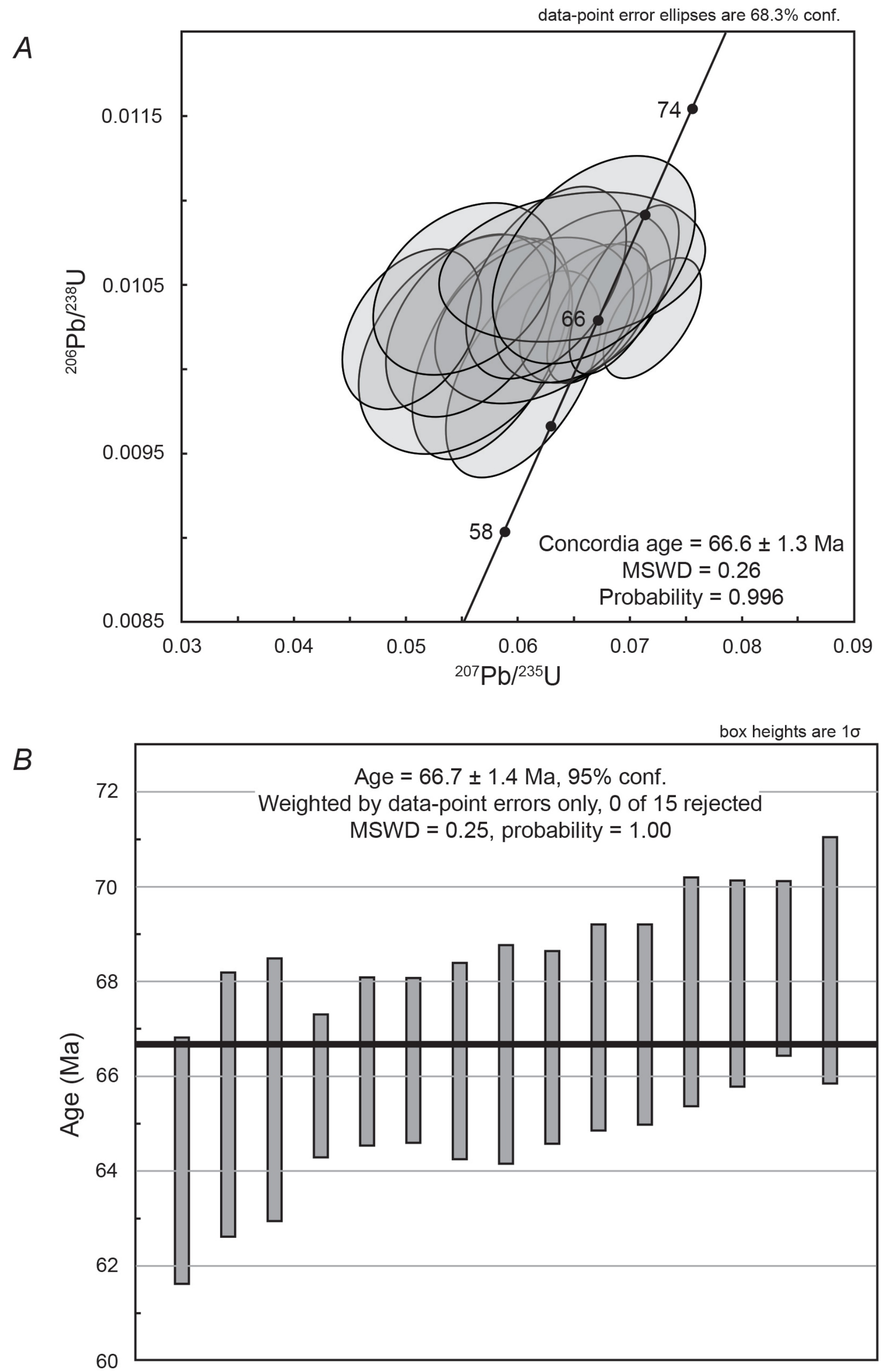

Figure 12. Uranium-lead (U-Pb) age data for zircons of sample 12WA31RT from the RPM mineral occurrence hosted within the Mt. Estelle pluton. *A*, Conventional concordia plot showing data for 15 zircon crystals. *B*, ^{207}Pb-corrected $^{206}Pb/^{238}U$ weighted-average age plot for the same zircons presented in part *A*. (Ma, millions of years ago [mega-annum]; MSWD, mean square weighted deviation; conf., confidence interval; σ, sigma [standard deviation])

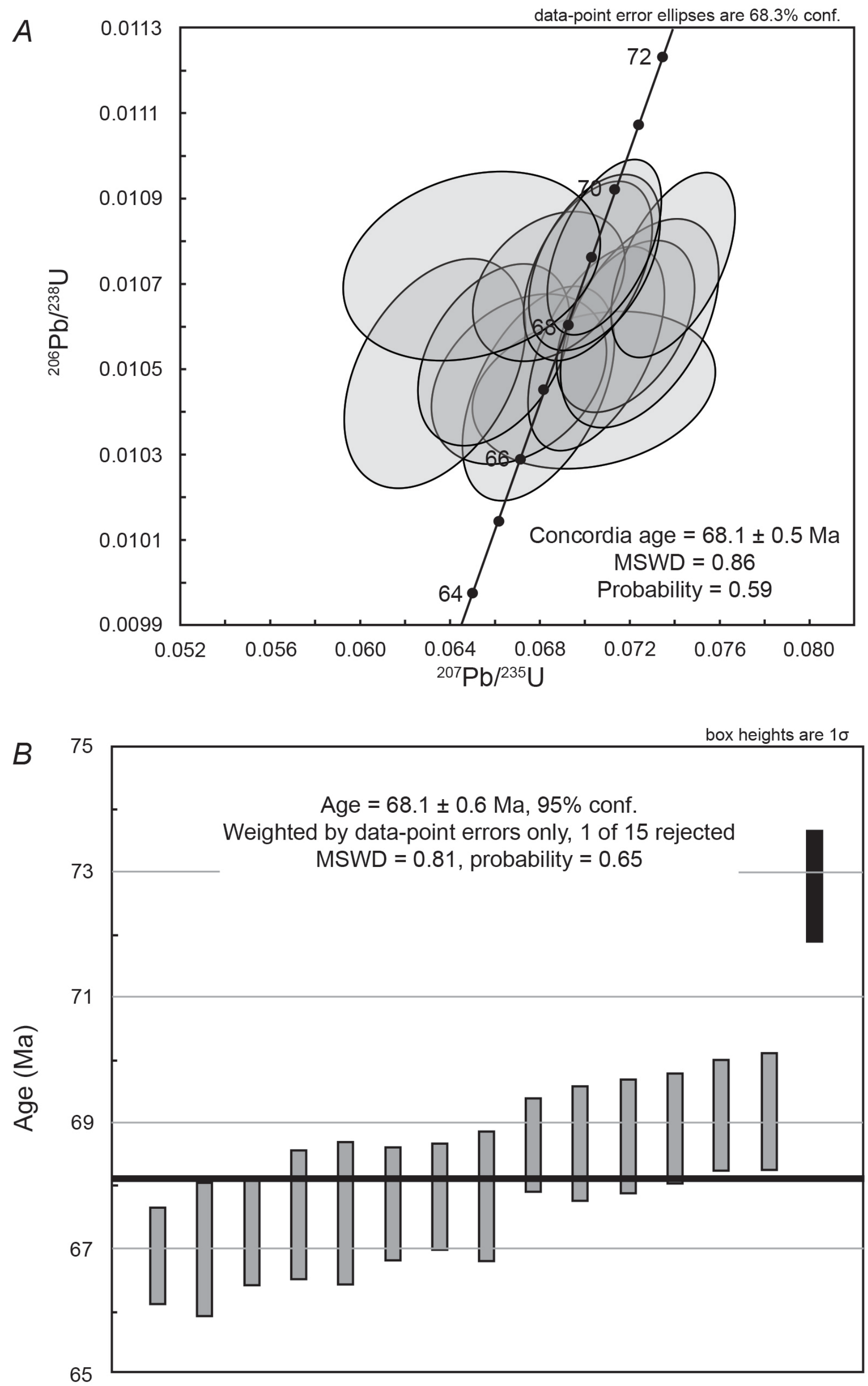

Figure 13. Uranium-lead (U-Pb) age data for zircons of sample 12WA33RT from the Oxide North mineral occurrence hosted within the Mt. Estelle pluton. *A*, Conventional concordia plot showing data for 14 zircon crystals. *B*, ^{207}Pb-corrected $^{206}Pb/^{238}U$ weighted-average age plot for the same zircons presented in part *A*. The black box represents an analysis that was rejected in the age determination. (Ma, millions of years ago [mega-annum]; MSWD, mean square weighted deviation; conf., confidence interval; σ, sigma [standard deviation])

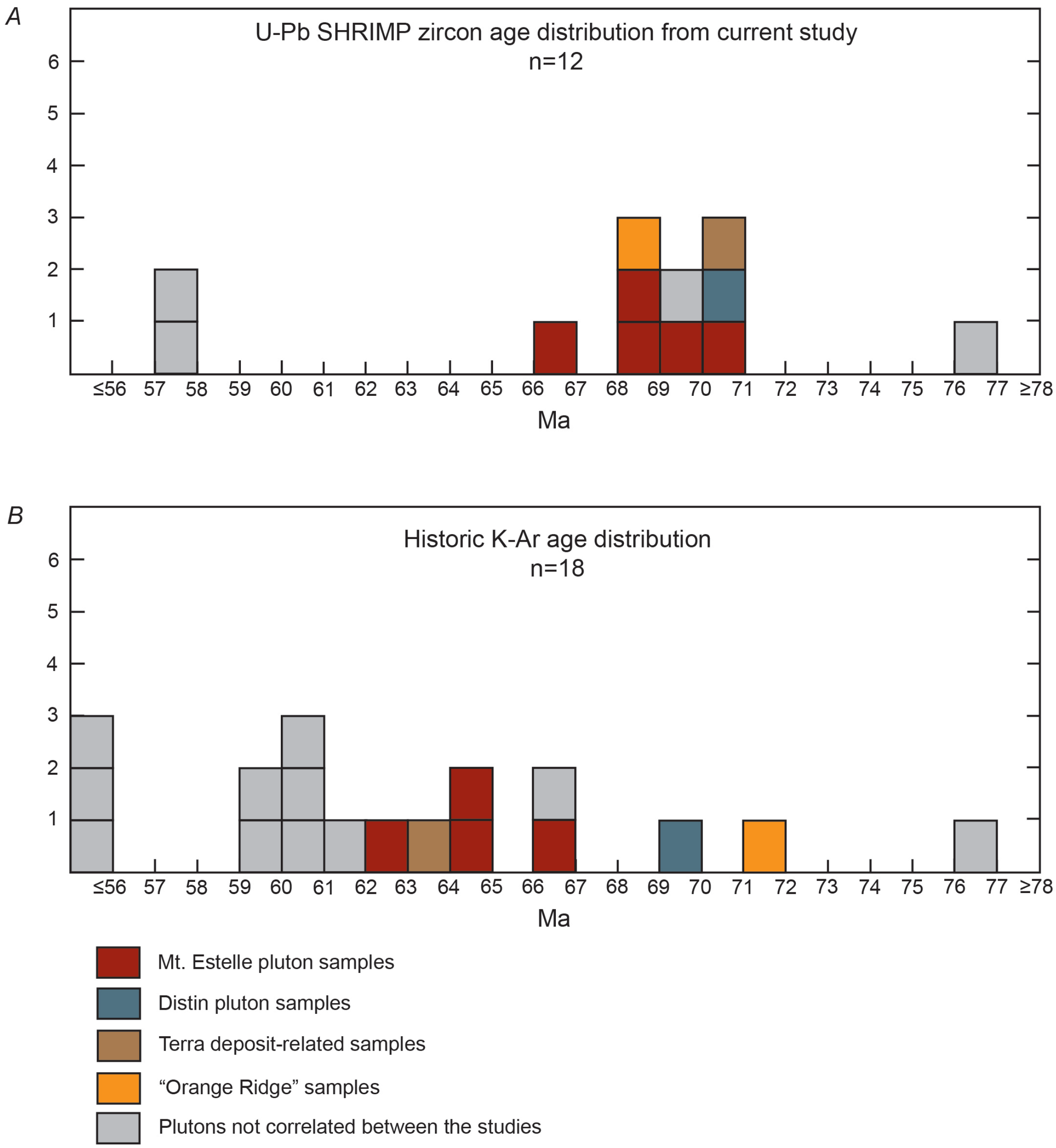

Figure 14. Age distribution histograms for plutons in the study area. Plutons dated by both methods are color coordinated. *A*, Uranium-lead (U-Pb) age distribution of plutons from this study. *B*, Potassium-argon (K-Ar) age distribution for plutons dated by Reed and Lanphere (1972, 1973). (SHRIMP, sensitive high-resolution ion microprobe)

Table 1. Locations of sample sites, analytical information, and summary of sample ages.

[Ma, millions of years ago (mega-annum); U, uranium; Pb, lead; Re, rhenium; Os, osmium. Latitude and longitude coordinates are given using the WGS 84 datum]

Location	Sample identification	Latitude	Longitude	Age[1] (Ma)	Error (Ma)	Mineral	Method
Mt. Estelle pluton—Oxide Valley	12WA01RT	62.0111	–152.9357	68.3	0.7	zircon	U-Pb
Mt. Estelle pluton—Train	12WA07RT	61.8261	–152.9251	70.1	1.2	zircon	U-Pb
Snow Ridge	12WA11RT	62.0062	–152.6866	76.6	0.8	zircon	U-Pb
Cristo	12WA13RT	61.7737	–152.3766	57.8	0.5	zircon	U-Pb
Distin pluton	12WA15RT	62.1119	–152.3497	70.6	0.6	zircon	U-Pb
Terra diorite	12WA17RT	61.7739	–153.7028	70.8	0.8	zircon	U-Pb
Old Man diorite	12WA25RT	61.9105	–152.3300	69.6	0.5	zircon	U-Pb
Mt. Estelle pluton—Muddy Creek	12WA26RT	61.8459	–152.8651	69.4	1.3	zircon	U-Pb
Jimmy Lake	12WA27RT	61.7428	–153.1935	57.4	1.7	zircon	U-Pb
Orange Ridge	12WA28RT	61.5731	–153.3142	68.0	1.1	zircon	U-Pb
Mt. Estelle pluton—RPM	12WA31RT	61.7725	–152.9627	66.7	1.4	zircon	U-Pb
Mt. Estelle pluton—Oxide North	12WA33RT	62.0237	–152.8981	68.1	0.6	zircon	U-Pb
Miss Molly	MM-11	61.7309	–152.0840	58.5	1.2	molybdenite	Re-Os

[1]Zircon ages are ^{207}Pb-corrected ^{206}Pb/^{238}U weighted-average ages of analyzed crystals.

Table 2. Sensitive high-resolution ion microprobe (SHRIMP) uranium-thorium-lead isotopic data for zircon crystals from plutons of the Alaska Range. (link to Excel file)

[U, uranium; Pb, lead; Th, thorium; ppm, parts per million; %, percent; Ma, millions of years ago (mega-annum); 4-corr, corrected for common ^{204}Pb; 7-corr, corrected for common ^{207}Pb; 8-corr, corrected for common ^{208}Pb; ρ, error correlation; strikethrough, data rejected for age calculations. Crystal identification derived from sample identification (table 1) by removing leading characters ("12WA") and appending a sequence number (-x)]

Table 3. Sensitive high-resolution ion microprobe (SHRIMP) trace element, titanium, and calculated temperature data for zircon crystals from plutons of the Alaska Range. (link to Excel file)

Table 4. Rhenium-osmium age data for the Miss Molly molybdenum occurrence.

[mg, milligrams; Re, rhenium; ppb, parts per billion; Os, osmium; Ma, millions of years ago (mega-annum)]

Sample identification	Weight (mg)	Re (ppb)	+/–	^{187}Re (ppb)	+/–	^{187}Os (ppb)	+/–	Age (Ma)	+/–
MM-11	25	141	2	89	1	67	1	58.5	1.2

Appendix. Photographs of Sample Sites

A, Comingled magma at Oxide Valley sample site. *B*, The Train prospect showing sampling site and the mineral prospect up and left from the sampling site. *C*, Rubble crop sample site at Snow Ridge. *D*, Sample site near the Cristo prospect. *E*, Distin pluton sample site. *F*, Boxes of drill core at the Terra deposit. *G*, Old Man diorite sample site. *H*, The Muddy Creek prospect with the outcrop and sample site circled. *I*, Sample of intrusive taken from the Jimmy Lake prospect with a large nugget of molybdenite. *J*, Looking down "Orange Ridge". *K*, The sharp ridge of the RPM prospect. *L*, Large boulders derived from the cirque headwall at Oxide North. Photographs *A*, *C*, *D*, *F*, *G*, *I*, and *L* taken by Ryan Taylor. Photographs *B*, *E*, *H*, *J*, and *K* taken by Garth Graham.

ISSN 2331-1258 (online)
http://dx.doi.org/10.3133/ofr20141115